



Aalborg Universitet

AALBORG UNIVERSITY
DENMARK

Laboratory Setup for Vertically Loaded Suction Caisson Foundation in Sand and Validation of Responses

Manzotti, E.; Vaitkunaite, Evelina; Ibsen, Lars Bo

Publication date:
2014

Document Version
Publisher's PDF, also known as Version of record

[Link to publication from Aalborg University](#)

Citation for published version (APA):

Manzotti, E., Vaitkunaite, E., & Ibsen, L. B. (2014). *Laboratory Setup for Vertically Loaded Suction Caisson Foundation in Sand and Validation of Responses*. Department of Civil Engineering, Aalborg University. DCE Technical Memorandum No. 41

General rights

Copyright and moral rights for the publications made accessible in the public portal are retained by the authors and/or other copyright owners and it is a condition of accessing publications that users recognise and abide by the legal requirements associated with these rights.

- Users may download and print one copy of any publication from the public portal for the purpose of private study or research.
- You may not further distribute the material or use it for any profit-making activity or commercial gain
- You may freely distribute the URL identifying the publication in the public portal -

Take down policy

If you believe that this document breaches copyright please contact us at vbn@aub.aau.dk providing details, and we will remove access to the work immediately and investigate your claim.

Laboratory Setup for Vertically Loaded Suction Caisson Foundation in Sand and Validation of Responses

**E. Manzotti
E. Vaitkunaite
L.B. Ibsen**



Aalborg University
Department of Civil Engineering

DCE Technical Memorandum No. 041

Laboratory Setup for Vertically Loaded Suction Caisson Foundation in Sand and Validation of Responses

by

E. Manzotti
E. Vaitkunaite
L.B. Ibsen

June 2014

© Aalborg University

Scientific Publications at the Department of Civil Engineering

Technical Reports are published for timely dissemination of research results and scientific work carried out at the Department of Civil Engineering (DCE) at Aalborg University. This medium allows publication of more detailed explanations and results than typically allowed in scientific journals.

Technical Memoranda are produced to enable the preliminary dissemination of scientific work by the personnel of the DCE where such release is deemed to be appropriate. Documents of this kind may be incomplete or temporary versions of papers—or part of continuing work. This should be kept in mind when references are given to publications of this kind.

Contract Reports are produced to report scientific work carried out under contract. Publications of this kind contain confidential matter and are reserved for the sponsors and the DCE. Therefore, Contract Reports are generally not available for public circulation.

Lecture Notes contain material produced by the lecturers at the DCE for educational purposes. This may be scientific notes, lecture books, example problems or manuals for laboratory work, or computer programs developed at the DCE.

Theses are monographs or collections of papers published to report the scientific work carried out at the DCE to obtain a degree as either PhD or Doctor of Technology. The thesis is publicly available after the defence of the degree.

Latest News is published to enable rapid communication of information about scientific work carried out at the DCE. This includes the status of research projects, developments in the laboratories, information about collaborative work and recent research results.

Published 2014 by
Aalborg University
Department of Civil Engineering
Sohngaardsholmsvej 57,
DK-9000 Aalborg, Denmark

Printed in Aalborg at Aalborg
University

ISSN 1901-7278
DCE Technical Memorandum No.
041

Laboratory Setup for Vertically Loaded Suction Caisson Foundation in Sand and Validation of Responses

E. Manzotti, E. Vaitkunaite, L.B. Ibsen

Aalborg University, Department of Civil Engineering, Denmark

Abstract: Wind energy obtained by means of wind turbine has been proved to be a concrete resource of green energy. Development of such structures requires research on offshore construction, since this is the direction for future improvement on this field. Wind turbines are relatively light and slender devices usually installed in farms, therefore many inexpensive foundations are needed. Suction Bucket foundations are a suitable option for this purpose, but for large scale utilization more research is required, especially for in-service performance. Size of offshore wind turbine has been increasing during the last years and, following this trend, design choice will turn into foundation composed of three or four suction bucket foundations, called respectively tripod and tetrapod. Overturning moment in tripod and tetrapod is carried by vertical loading, therefore vertical pull-out capacity is tested, in both static and cyclic case of loading. Testing rig and equipment are presented together with procedures. Tests results are presented in order to verify the output of tests. CPT-based methods and beta-methods to evaluate installation and pull-out resistance are then presented and implemented in Matlab in order to validate responses. It is demonstrated that k_f parameter of CPT-based methods is dependent on the overburden pressure applied. Parameters of beta methods are analyzed and defined. Satisfying results are obtained with methods that are considering a linear increase or decrease with the depth of vertical stress, depending if the case of application is installation or pull-out.

1. INTRODUCTION.

Nowadays wind turbines have been proven to be a reliable source of ‘green energy’. Onshore installations are present but not always possible, because of the impact on the landscape and large areas required. Wind turbines are therefore preferably installed offshore, where larger structures can be realized, and more stable wind allows a more regular production (Byrne *et al*, 2003). A drawback of offshore installations is the greater load given by wind and waves, and the installation procedure, although the latter can cause problems also in onshore installation.

Such light structures like wind turbines, are subjected to small vertical load, compared to the overturning moment caused by waves and wind. Wind turbines are usually founded on piles. This typology of foundation is well known and of simple design, but is considered expensive, since represents the 35% of the total cost of the installed structure (Byrne *et al*, 2003). Cost is always an important issue, especially for offshore wind turbine that has been shown to be a reliable source of renewable energy with a great potential of expansion in the market. Suction caisson foundation, also called suction bucket foundation, is an alternative solution for offshore foundations. Alternative that allows to decrease the total cost of the structure, requiring less material and less cost in terms of construction and installation, compared to pile foundation.

A suction caisson foundation has the shape of an upturned bucket, with an aspect ratio, length over diameter (L/D), less than one for structures installed in sand. The installation consists of two main steps: first, the foundation penetrate the soil under its own weight, then suction is applied, reducing the pressure inside the bucket, and allowing the complete insertion of the caisson into the soil.

In light and slender structures such as wind turbine, horizontal load in extreme condition may reach 60% of the vertical load (Houlsby *et al*, 2005c), making overturning moment on the foundation the main concern. Bucket foundations are installed both as monopod (single structure) or tripod/tetrapod (multiple foundation). In the first case overturning moments are resisted directly by the rotational capacity of the foundation, in the second case overturning moments are transmitted to the foundation by transient tension and compression vertical loads, on the respectively upwind and downwind legs. The accumulated deformation under cyclic loading is the main issue of interest during design of both monopod and tripod/tetrapod, since can brings to serviceability problems (Byrne *et al*, 2003; Kelly *et al*, 2005).

In general, physical models are an approximation of real natural condition, given that a laboratory set up is always subjected to laboratory effects and scale effects. Laboratory effects are due to the difficulty of reproducing the physical

condition found in nature, as environment surroundings and loads. To overcome this problem, the sand box used in tests presented in this article has dimensions designed in a way that does not interfere with the bucket installed in its centre, and therefore gives a faithful reproduction of seabed. Scale effects increase increasing the scale factor, since quantity that cannot be scaled such as gravity, viscosity, grain size, etc. affect results of scaled quantities. The equipment of Aalborg University laboratory has a scale factor approximately of 1:10, allowing low scale effects.

Testing setup presented in this article, is made to investigate the behaviour of foundations subjected to vertical loads in sand. In this work, only procedures to test bucket foundations are discussed, despite that, the system is suitable also for other typologies of foundations, such as monopiles. By MOOG program a wide range of static and cyclic loads can be applied, and the sand box equipment allow to apply overburden pressure by suction. In the case of study only tensile vertical loads will be applied, with and without overburden pressure. Therefore typical loads to which are subjected the upwind legs of a multiple foundation is simulated.

In literature, various design methods has been proposed in order to evaluate installation and pull-out resistance of suction caisson in sand. In this study, responses from installation and pull-out tests carried out at Aalborg University are utilized to compare results from different methods. Effect of suction is not considered because this phenomenon is not present during installation and has a marginal importance on pull-out response in drained condition. Beta-methods and CPT-based methods of interest are presented. Then methods are analyzed and validate, grounding on experimental responses.

2. EQUIPMENT.

Tests are carried out in the geotechnical laboratory of Aalborg University, structure of the equipment used is shown schematically in *Figure 1*.

The testing rig includes a rigid circular box, a movable loading frame equipped with two movable hydraulic pistons, a signal transducers box and a measuring system described in the following.

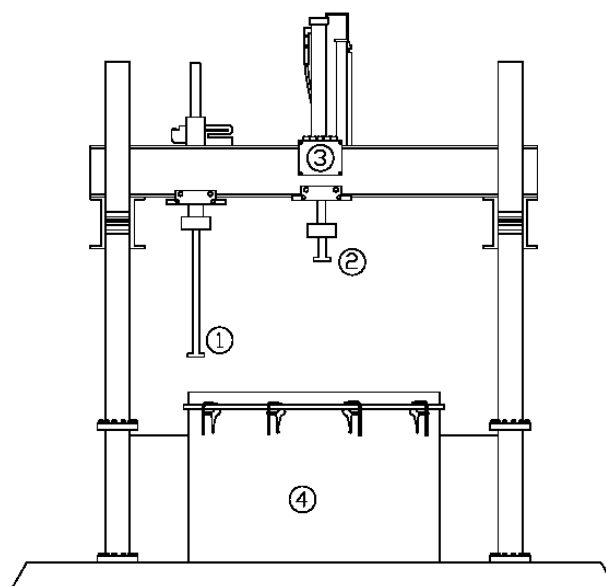


Figure 1. Equipment used testing bucket foundation: loading piston (1), installation piston (2), signal transducers box (3) and sand box (4).

Testing system shown in *Figure 1* is described together with equipment for specific testing of bucket foundation.

2.1 Sand box

The sand box is a steel made cylinder with a diameter of 250 cm and a total height of 152 cm. A 30 cm thick layer of gravel with high permeability is placed at the bottom, in order to provide a uniform distribution of water and create uniform water pressure, avoiding piping problems. A geotextile sheet is placed on top of the gravel layer, to avoid sand infiltration and thus maintain drainage property unaltered. The top layer is composed of Aalborg University Sand No.1 and has a thickness of 120 cm. Water is leaded into the box by a system of perforated pipes, uniformly placed on the bottom.

To supply water a tank of 1 m³ is filled of water and placed in a higher position with respect to the sand box. This allows having an upward gradient in the sand box, needed to loosen the sand. The in and out flow of water is controlled by a system of valves shown in *Figure 2*. Regulating the inflow valve, the level of gradient in the sand box is regulated and measured with a piezometer, on which a mark is made in order to have a gradient of 0.9.



Figure 2. In and out flow valves.

2.2 Bucket Models.

Two cylindrical shaped models of bucket foundation have been built to be tested. Both models have an outer diameter of 1000 mm, and a wall thickness of 3 mm, the skirt length is 500 mm for M1 (aspect ratio $L/D=0,5$), and 1000 mm for M2 ($L/D=1$). Models are approximately scaled of 1:10.

Each model is composed of two parts. The first component is a steel made bucket, with a thickness of 3 mm, the second component is a steel plate placed above the lid of the bucket, with a thickness of 20 mm (Figure 3). The steel plate is connected to the bucket by eight bolts and a rubber gasket is installed along the diameter, this connection is made to make possible to place the elastic membrane in between, when a test with suction is run.

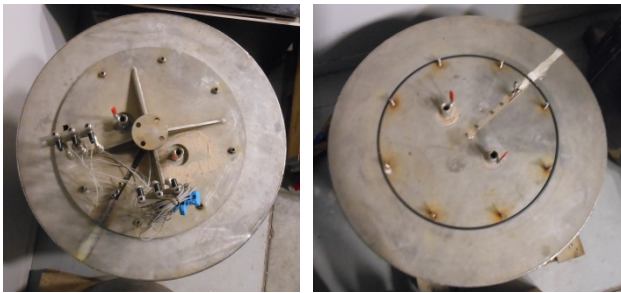


Figure 3. Bucket model with steel plate installed (left) and without steel plate (right).

2.3 Suction equipment

To simulate overburden pressure the sand is compressed by a suction system that create a depression inside the sand box.

Hermetic isolation is provided by a membrane made of non-porous latex rubber. The membrane has been cut so that can fit with the bucket model, it has a thickness that allow it to adapt to the sand surface. Four connection for suction pipes and one connection for surface pressure transducer are installed on the membrane.

Hermetic isolation along the perimeter of the sand box is provided by a groove where a circular rubber gasket is inserted. The membrane is stretched on the rubber gasket and the steel frame is placed on it and fixed with clamps (Figure 4).



Figure 4. Membrane fixed.



Figure 5. Suction Tank.

Suction tank (Figure 5) has a capacity of 320 liters, is provided of a barometer and is connected with the compressed air system of the laboratory. To activate the suction, both compressed air valve and the valve of the tank have to be opened. At this point suction starts and measures of pressures are sampled by Catman.

2.4 Loading and measuring systems.

Two hydraulic pistons are connected on the frame placed above the sand box: the installation piston and the loading piston (Figure 1).

Installation piston is used to run CPT tests and to install the bucket. It has a capacity of 200 kN and is actuated by a control, while speed has to be settled by the control panel in a range of 0.01-5 mm/s. Vertical displacement is measured by a displacement transducer connected to the transducers box, applied force is measured by a load cell. The signals are recorded by a computer with the program Catman.

Loading piston can apply a vertical force of 250 kN and has a maximum displacement range of 40 cm. Force or forced displacement for static and cyclic loading are applied with loading piston, controlled by the MOOG system whereby data are recorded and test are programmed. A wide range of options are available for cyclic loading in terms of frequencies and load modalities. Displacements are measured by two 125 mm displacement transducers, installed on a horizontal bar fixed at the side of the box, and connected to specific nuts installed at two opposite sides of the bucket (Figure 6). Displacement sensors are connected to the relative channels in the transducer box, signals are then elaborated and registered by MOOG system.



Figure 6. Displacement transducers WS10-1 and WS10-2 connected to the horizontal bar.

As shown in Figure 7, six pressure transducers are installed at different levels inside and outside the bucket. Installation valves and connection for pressure transducers are installed on top of the lid. Cable of pressure transducers are connected to the signal transducers box and through the signal amplifier MGCplus and Spider 8, the signal is elaborated by Catman.

vibrator is made to ensure to reach a depth of 60 cm in case of M1 bucket or 110 cm in case of M2 bucket. During vibration it is important to keep the rod vibrator as perpendicular as possible and maintain a constant slow velocity in order to have a uniform vibration and allow the air to come out. After vibration the outflow valve is opened and water level is lowered till one centimeter above the sand surface, then the wooden plates are removed and the surface is first cleaned manually, then levelled using a specific shaped aluminium beam.

3.1 CPT tests

Cone penetration tests are carried out to have complete information about compaction and homogeneity of the soil.

CPT probe used is shown in *Figure 10*. It has a diameter of 15 mm, tip area of 176.7 mm, cone angle of 60° and penetration length of 120mm. It is connected to the installation pistons then force transducer is plugged in the signal transducer box. Afterwards four CPT tests in four different positions are run, moving and fixing each time the installation piston in the corresponding position, each position is marked by the corresponding number on the inner side of the transverse IPE profile.

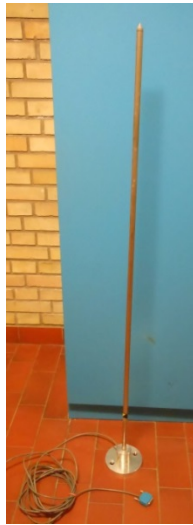


Figure 10. CPT probe.

The penetration velocity has to be settled on 5 mm/s, then the piston is activated and stopped at the sand surface. At this point Catman program is reset and then run registering data of the penetration resistance q_c , time and vertical displacement. The installing piston is activated until a depth of 110 mm, to help on this step, a yellow tag is attached on the probe.

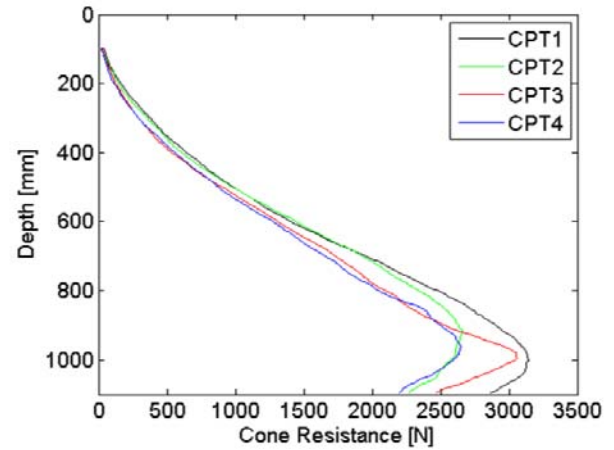


Figure 11. CPT test results for test n°5

In *Figure 11* shows the typical results of cone penetration test made in the four positions of the test rig. Trend of the curves shows a cone resistance that uniformly increases with depth till a depth of approximately 600 mm. This is a satisfactory soil preparation for a M1 Bucket test, since depths of interest are from 0 to 500 mm.

Figure 12 shows the variation in relative density with respect to depth. Iterative process to calculate D_r is described in *Ibsen et al. (2009)*.

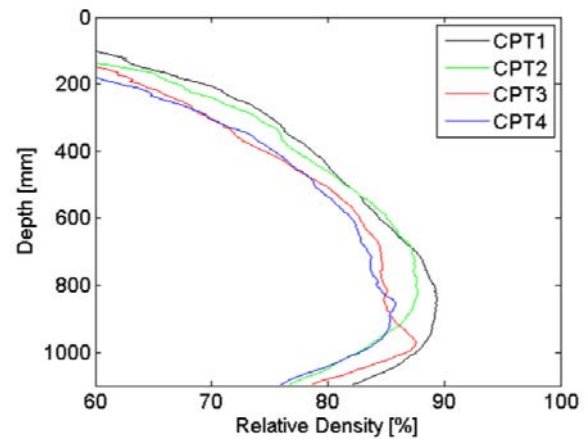


Figure 12. Relative density for test n°5.

3. TEST PROCEDURES.

In the following, steps on how to run tests are described. Soil preparation is common for both tests with and without membrane. Steps of installation are the same for both long and short bucket. Only differences are the longer time and greater preloading force required in the installation of long bucket M2.

3.1 Test without membrane

The water level is raised till 5-8 cm above the surface level, and so is kept while tests are run. The bucket is prepared first blowing out the sand from pipes of pressure transducers. Pipes are filled with water by immersing the bucket in a water box and, using suction equipment, water is sucked inside pipes (*Figure 13*). During this phase check that pipes are completely full of water and no bubble air are present.



Figure 13. Bucket immersed in the water box.

The bucket is connected to the installation piston and speed is set on 0.2 mm/s. Before to activate the piston, installation valves have to be opened and Catman run to register loading and displacement data. Despite the low speed, such installation does not reproduce all phenomena happening during the real installation. On the field installation suction is applied and a flow is created around the skirt, helping the penetration.

To ensure comparability between different tests, a preloading load of 70 KPa is reached before to close the two valves of the lid. An indicator of a good installation is water flowing out from the two valves of the lid, since no air is trapped between lid and soil.

Figure 14 is showing installation loading curve that is similar for all tests, since sand and sand properties like relative density and saturation are uniformed by soil preparation. In the first part of the curve it can be seen the increase of resistance due to skin friction of the sand adjacent to the caisson. When the lid touches the surface, the load is let to increase till 70 kN.

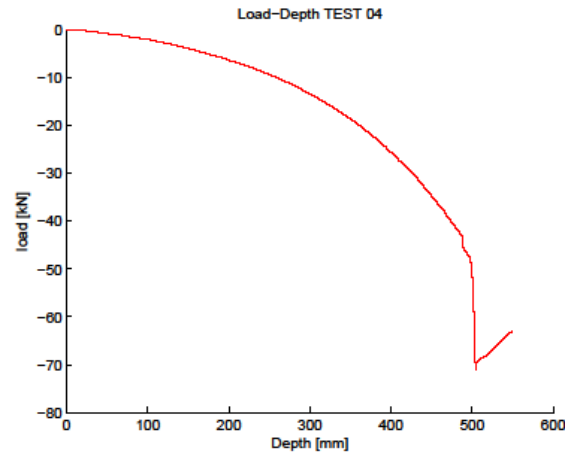


Figure 14. Installation load curve for static test.

Once installation has been completed, installation piston is disconnected and activated with an upward speed velocity of 0.2 mm/s, in order to limit disturbance to the installed bucket. Despite this precaution a slight bump of the lid of the bucket is unavoidable, this is due to the bending of the bucket lid happening during installation process.

Loading piston is positioned in the central position of the horizontal beam and fixed with 8 bolts. To connect the loading piston with the bucket, a light safety limit of the force has to be set in MOOG, so when the two parts start touching each other the system automatically stops, and the four bolts of the connection can be fixed.

Pressure sensors are connected to the signal transducers box. Data of pressures, load and displacement are registered by both MOOG and Catman.

3.2 Test with membrane

To simulate overburden pressure test with membrane have to be set. Overburden pressure is simulated in order to have a greater value of stress at the level of the lid. This allows simulating a bucket with longer skirt, and so applying a bigger scale. A drawback of suction is that also water is aspirated out of the sand box, so the sand layer is not fully saturated.

To start the test, first the bucket is prepared fixing the membrane under the steel plate of the bucket as shown in *Figure 15*. Preparation and installation of the bucket are then the same as described in *section 3.1*.



Figure 15. Membrane fixed under the lid.

After the bucket is penetrated into sand, the filter is laid on the sand and the membrane is outstretched so that overlay the rubber gasket placed on the perimeter. A metal ring is positioned and fixed with clamps. Installation piston is then removed and load piston is connected as indicated in the procedure of without membrane test.

Suction pipes are connected to the membrane and the suction system is activated. The pressure level is measured by Catman and, once reached the required value, has to be kept constant for at least 12 hours.

4. RESULTS PRESENTATION.

Tests carried out on this work are summarized in Table 2

Test	L/D	Load	Overburden pressure [kPa]	Displacement [mm]	Amplitude [kN]
13.02.06	0.5	Static	0	3.8	-
13.02.08	0.5	Static	0	4	-
13.02.09	0.5	Static	40	8.8	-
13.02.10	1	Static	0	3.9	-
13.02.11	0.5	Static	20	4	-
13.02.12	0.5	Static	40	6	-
13.02.14	1	Static	0	6.5	-
13.02.15	0.5	Static	0	4	-
13.03.02	0.5	Cyclic	0	-	1.925
13.03.03	0.5	Cyclic	0	-	3.85

Table 2. Test overview.

In the following is shown how results can be presented. A MATLAB code has been created so that data can be elaborated and plotted. All tests presented are carried out

with the bucket model M1 ($L/D=0.5$) numbers in Figure 16 are showing the corresponding position of pressure measurements.

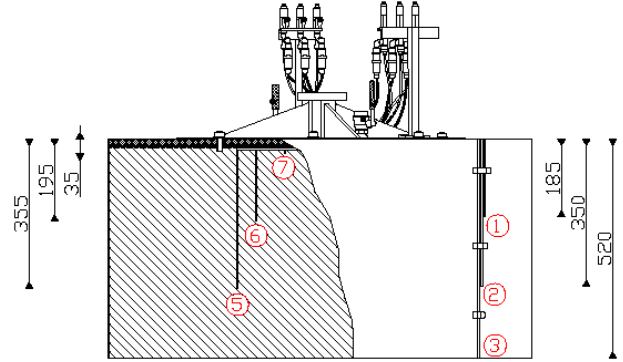


Figure 16. Position of pressure measurements.

4.1 Static test without suction

Figure 17 is shown the expected trend for a static load-displacement curve. In this case in MOOG it has been set up a vertical displacement of 60 mm that has to be reached in 3000 seconds. The load is suddenly increasing reaching a value of 7.8 kN, than is slightly decreasing till a value of 6.2 kN before to drop in correspondence of the end of the test.

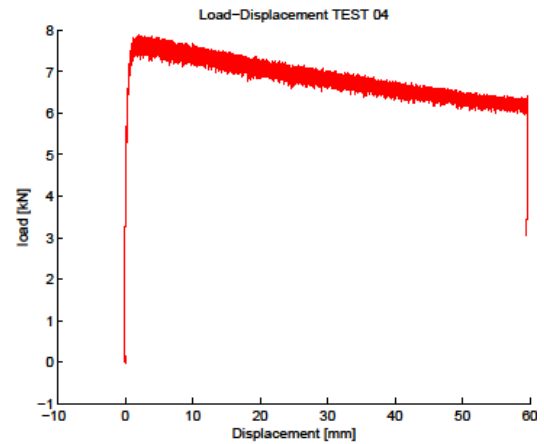


Figure 17. Load-Displacement curve for static test.

To show pressure measurements, it has been chosen to split the results in two graphs. In Figure 18 and Figure 19 measures respectively inside and outside the bucket model are shown. Measurement of atmospheric pressure given by "p6a" channel is shown in both graphs, this is made in order to have a reference point and allow a better comparison between results.

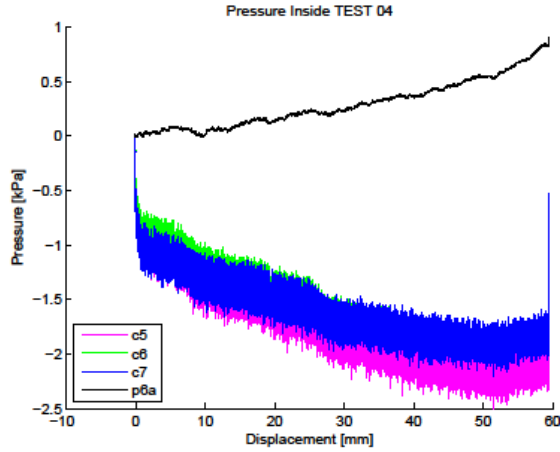


Figure 18. Pressure measurements inside the bucket.

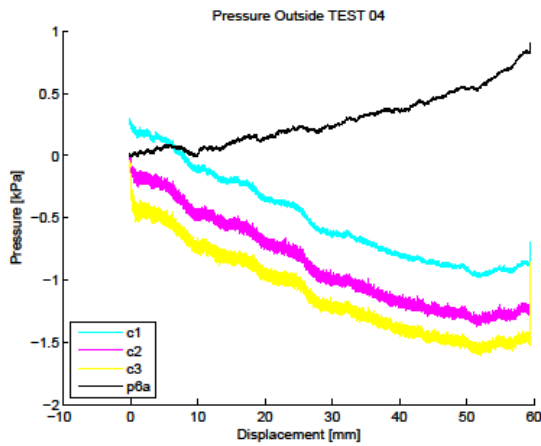


Figure 19. Pressure measurements outside the bucket.

4.2 Cyclic test without suction

Figure 20 shows a load-displacement curve for a cyclic test. Considering results of static test, for the cyclic test 40000 cycles has been settled with a frequency of 0.1 Hz and an amplitude of 50% of the static maximum load. Before of the cyclic load, the bucket is loaded with a static tensional load of 50% of the static maximum load, by “round ramp” mode.

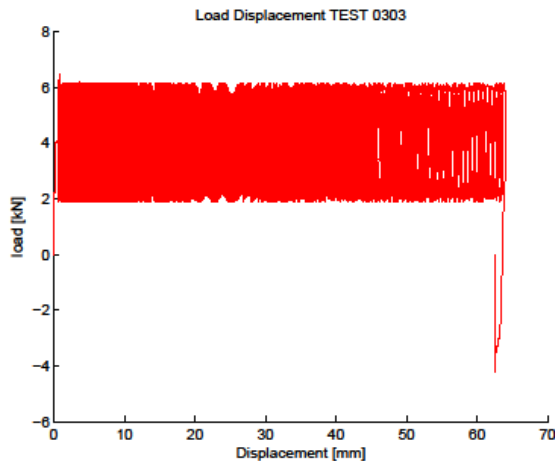


Figure 20. Load-Displacement curve for cyclic test.

Pressure results are presented in the same way as for the static test, as can be seen in Figure 21 and Figure 22. Pressure measurements presents a wide fluctuation so, in order to have a more clear plots of results, a “reduced plotting” function has been used in the MATLAB code.

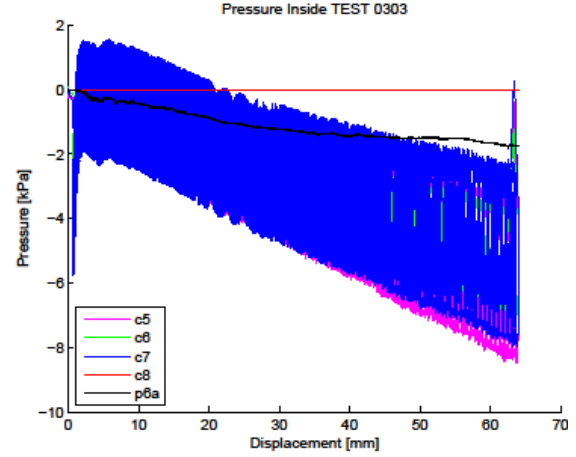


Figure 21. Pressure measurements inside the bucket.

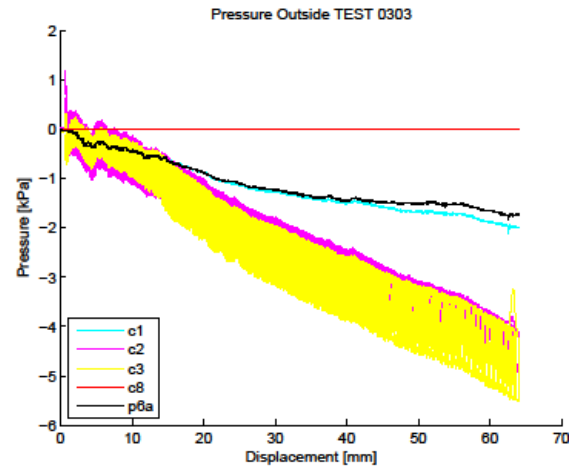


Figure 22. Pressure measurements outside the bucket.

5. VALIDATION OF RESULTS.

Methods presented in this work are divided in CPT based methods and beta-methods, based respectively on cone resistance and $\beta = K \tan \delta$. Effect of suction is not considered, since this phenomenon is not present in test used to validate results.

Methods to calculate pull-out resistance without considering passive suction are representing response of a totally drained behavior, where drainage conditions does not allow pore pressure to build up. In these methods only frictional resistance is taken into account.

To compare installation methods, the weight of the caisson is not considered, since piston used for installation has been

reset to zero value with the caisson connected. The skirt-soil friction angle δ is kept constant to a value of 30° , since this is the most suitable value for very dense sand in contact with steel, as confirmed in Table 2-1 in *Senders (2008)*.

Installation of a bucket foundation carried out by pushing, requires more force than installation where active suction is applied. The negative pressure, in non-cohesive soils, is helping installation creating a flow from outside to inside the caisson that, acting on friction resistance, results in a beneficial effect for skirt penetration.

In order to compare results, load and displacements are plotted in dimensionless form, respectively as $V/(D^3 \gamma)$ and h/D , according to *Kelly et al. (2006)*. In the following study, parameters are evaluated from responses of test 6, test 9, and test 11, carried out with overburden pressure of respectively 0kPa, 40kPa, and 20kPa.

5.1 Beta methods.

Installation beta methods (Houlsby et al. 2005a).

In *Houlsby et al. (2005a)*, it is reported a method to evaluate the pushing installation resistance of a suction caisson following the conventional pile design practice. The suction caisson is modelled as an open-ended pile, having the tip area equal to the thickness of the skirt. Installation resistance is evaluated as the sum of end-bearing resistance, friction outside the skirt and friction inside the skirt, as shown in the *Formula 1*.

$$V' = \frac{\gamma' h^2 (K \tan \delta) (\pi D_o)}{2} + \frac{\gamma' h^2 (K \tan \delta) (\pi D_i)}{2} + (\gamma' h N_q + \gamma' h N_\gamma) (\pi D t) \quad (1)$$

This method is unconservative, as stated in *Houlsby (2005a)*, given that is not taking into account the enhancement given by friction to the vertical stress next to the skirt.

The increase of vertical stress with the depth considering enhancement given by skin friction, is calculated in *Houlsby (2005b)*, making equilibrium of vertical forces on a disc of soil adjacent to the skirt, where also soil-caisson frictional forces are taken into account. Other two methods are presented, where the enhancement given by skin friction to vertical stress is considered constant or linearly increasing with the depth, respectively for the second and third method presented.

In the second method the equilibrium of vertical forces inside the skirt is made considering width of the disc is equal to the internal diameter, whereas outside the skirt, width of the disc is governed by parameter m . Therefore the whole internal plug and a constant section outside the skirt are affected by the enhancement in vertical stresses. *Formulae 2 and 3* are solutions of the equilibrium for, respectively, internal and external vertical forces.

$$\frac{d\sigma'_{vi}}{dz} = \gamma' + \frac{\sigma'_{vi}}{Z_i} \quad (2)$$

$$\frac{d\sigma'_{vo}}{dz} = \gamma' + \frac{\sigma'_{vo}}{Z_o} \quad (3)$$

Where

$$Z_i = \frac{D_i}{(4(K \tan \delta)_i)} \quad (4)$$

$$Z_o = \frac{D_o(m^2 - 1)}{(4(K \tan \delta)_o)} \quad (5)$$

If *Formula 6* is verified, end bearing stress is calculated with *Formula 7*

$$\sigma'_{vi} - \sigma'_{vo} < \frac{2tN_\gamma}{N_q} \quad (6)$$

$$\sigma'_{end} = \sigma'_{vo} N_q + \gamma' \left(t - \frac{2x^2}{t} \right) N_\gamma \quad (7)$$

Where

$$x = \frac{t}{2} + \frac{(\sigma'_{vo} - \sigma'_{vi}) N_q}{4\gamma' N_\gamma} \quad (8)$$

If *Formula (9)* is verified, then $x = 0$ and the end bearing resistance is evaluated by *Formula (10)*.

$$\sigma'_{vi} - \sigma'_{vo} \geq \frac{2tN_\gamma}{N_q} \quad (9)$$

$$\sigma'_{end} = \sigma'_{vo} N_q + \gamma' t N_\gamma \quad (10)$$

In the method proposed by *Houlsby (2005a)*, the vertical load on the caisson for penetration to depth h is given by *Formula 11*.

$$V' = \gamma' Z_o^2 \left(e^{\frac{h}{Z_o}} - 1 - \frac{h}{Z_o} \right) (K \tan \delta) (\pi D_o) + \gamma' Z_i^2 \left(e^{\frac{h}{Z_o}} - 1 - \frac{h}{Z_o} \right) (K \tan \delta) (\pi D_i) + \sigma'_{end} \quad (11)$$

The third method presented is considering a linear increase of the enhanced vertical stress with the depth. The rate of change on the inside and on the outside of the bucket is given respectively by constants f_i and f_o . Therefore *Formulae 4 and 5* are substituted with *Formulae 12 and 13*

$$Z_i = \frac{D_i \left\{ 1 - \left[1 - \left(\frac{2f_i z}{D_i} \right) \right]^2 \right\}}{(4(K \tan \delta)_i)} \quad (12)$$

$$Z_o = \frac{D_o \left\{ \left[1 + \left(\frac{2f_i z}{D_i} \right)^2 \right] - 1 \right\}}{(4(K \tan \delta)_o)} \quad (13)$$

Then forces are calculated solving *Formulae 2* and *3* with a fourth order Runge-Kutta method. Due to the way of which Z_o is evaluated, the third beta method cannot be applied to suction caisson with $L/D=1$ or greater.

Pull-out beta methods.

Methods presented in *Houlsby (2005b)*, are calculating pull-out friction resistance summing internal and external friction on the skirt. It is assumed that the soil immediately breaks the contact with the lid of the caisson, furthermore effective stresses along the bottom rim of the skirt are considered negligible.

Two methods are presented. The linear method is calculating the friction resistance summing internal and external friction following the conventional pile design practice (*Formula 14*).

$$V' = \frac{-\gamma' h^2 (K \tan \delta) (\pi D_o)}{2} + \frac{-\gamma' h^2 (K \tan \delta) (\pi D_i)}{2} \quad (14)$$

Second method is taking into account the reduction in vertical stress given by the friction further up the skirt (*Formula 15*). On the internal side of the skirt, all the plug is affected by stress reduction. On the outside of the skirt a parameter m is defining the zone of stress reduction. Therefore internal and external friction are calculated considering uniform stress, and the zone of vertical stress reduction is assumed constant along the skirt.

$$V' = \gamma' Z_o^2 y \left(\frac{h}{Z_o} \right) (K \tan \delta) (\pi D_o) + \gamma' Z_i^2 y \left(\frac{h}{Z_i} \right) (K \tan \delta) (\pi D_i) \quad (15)$$

Where

$$y(x) = e^{-x} - 1 + x \quad (16)$$

In both methods it has to be checked that the internal friction resistance does not exceed the weight of the soil plug inside the caisson, this condition is expressed by *Formula 17*.

$$\frac{\gamma' h \pi D_i^2}{4} > \int_0^h \sigma'_{vi} (K \tan \delta) (\pi D_i) dz \quad (17)$$

5.2 CPT-based methods.

DNV CPT-based installation method.

DNV presents a method to estimate the installation resistance of steel caisson based on the average cone resistance q_c . End-bearing resistance and friction resistance on the skirt, are related to q_c respectively by constants k_p and k_f , of which suggested ranges are listed in *Table 3*.

k_p		k_f	
Most probable	Highest expected	Most probable	Highest expected
0.3	0.6	0.001	0.003

Table 3. Parameters suggested by DNV.

Installation resistance is calculated summing friction forces and end-bearing resistance by *Formula 18*.

$$V_{in} = F_i + F_o + Q_{tip} \quad (18)$$

Where internal friction, external friction and end-bearing resistance are given respectively by *Formulae 19, 20, 21*.

$$F_i = A_{si} k_f \int_0^h q_c(z) dz \quad (19)$$

$$F_o = A_{so} k_f \int_0^h q_c(z) dz \quad (20)$$

$$Q_{tip} = A_{so} k_p q_c(z) \quad (21)$$

A_{si} and A_{so} are respectively the inner and outer caisson perimeter, calculated as $A_s = D\pi$ inserting D as inner or outer diameter depending on the case.

Senders (2008) CPT-based installation method.

Senders (2008) suggests to modify CPT-based method presented in DNV using a different k_p and evaluating k_f with *Formula 22*.

$$k_f = C * \left(1 - \left(\frac{D_i}{D_o} \right)^2 \right)^{0.3} * \tan \delta \quad (22)$$

Where $C=0.21$ is a constant suggested by *Lehane et al. (2005)*.

k_p factor is taking into account differences in shape between the circular cone and the strip geometry of the caisson rim. Values of the shape factor s_q , giving the ratio between N_q for circular and strip footing, have been extrapolated and are showed in *Figure 23*, where are plotted with respect to the friction angle. In *Senders (2008)* it was noticed that s_q factor is in line with the range of k_p factor suggested by *DNV*, and s_q was therefore substituted to k_p in the calculation.

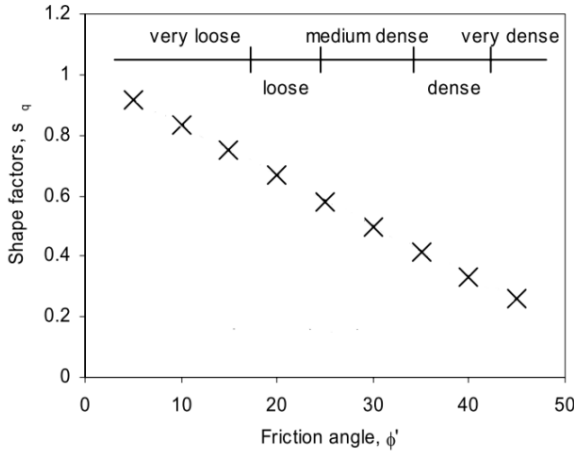


Figure 23. Theoretical shape factor (Randolph 2004).

In the present work it is chosen to use $k_p = s_q = 1 - 0.016\phi' = 0.1536$.

CUR pull-out CPT-based method.

Method suggested by *CUR* introduces a constant $k_f = 0.004$ *Senders (2008)* to evaluate the frictional pull-out resistance from q_c . In *CUR* is also presented a CPT based method to evaluate penetration resistance, where higher value of k_f is utilized. Therefore in *CUR* it is pointed out that friction resistance in compression is higher than friction resistance in tension. Friction resistance in drained condition is calculated by *Formula 23*.

$$V_{out} = F_i + F_o \quad (23)$$

In the method suggested by *CUR*, internal and external friction are given respectively by *Formula 24* and *Formula 25*.

$$F_i = -A_{si} k_f \int_0^h q_c(z) dz \quad (24)$$

$$F_o = -A_{so} k_f \int_0^h q_c(z) dz \quad (25)$$

Senders CPT-based pull-out method.

Senders (2008) proposed a CPT based method where friction resistance is calculated following *CUR* procedure, but a different value of k_f is introduced (*Formula 26*). k_f from compressive capacity is corrected considering the ratio between tensile and compressive friction. This ratio was extrapolated from experimental results in centrifuge tests by *Senders (2008)*, as -0.375 , therefore is reducing pull-out friction resistance with respect to installation friction resistance. In the present work, the ratio between tensile and compressive friction is evaluated from back-calculation and experimental responses as -0.1652 , and is substituted to -0.375 in *Formula 26*.

$$k_f = -0.1652 C \left(1 - \left(\frac{D_i}{D_o} \right)^2 \right)^{0.3} \tan \delta \quad (26)$$

5.3 Validation of CPT-based methods.

Validation of installation CPT-based methods.

In order to show how different value of k_f are affecting results of CPT-based methods, in *Figure 24* are plotted responses keeping constant $k_p=0.3$, while k_f is varying on the range proposed in *DNV (Table 3)*.

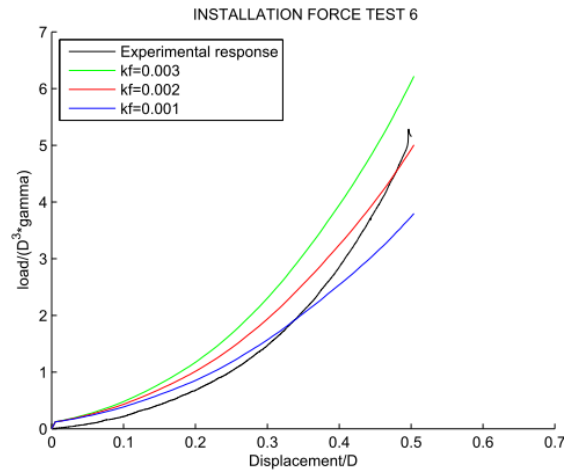


Figure 24. DNV method with constant $k_p=0.3$ while k_f is varying.

Figure 25 is showing the effect on the response varying k_p in the range suggested by *DNV*, and maintaining constant $k_f=0.002$. As can be noticed from *Figure 24* and *Figure 25*, increase of the response is directly proportional to k_f and k_p .

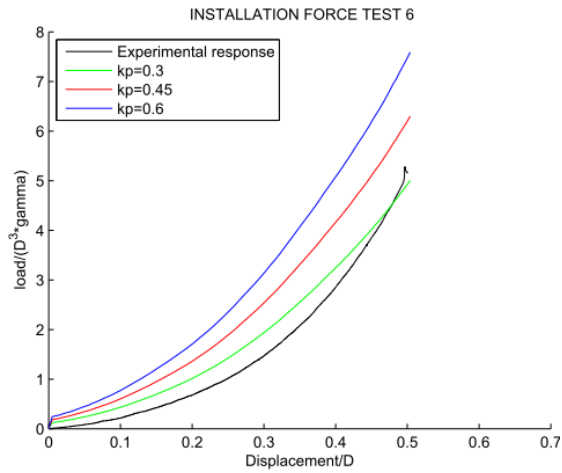


Figure 25. DNV method with constant $k_f=0.002$ while k_p is varying.

Parameters of method suggested by *Senders (2008)* are evaluated as $k_f=0.0032$ (Formula 19), and $k_p=0.1536$ (Figure 23). Best fit of parameters in DNV method is obtained with $k_f=0.002$ and $k_p=0.3$. Responses are shown in Figure 26.

Both CPT-based methods are giving a good approximation of the experimental response, as can be seen from Figure 26. Peak of the experimental response is $4.92D^3\gamma'$, peaks in *Senders (2008)* and DNV methods are, respectively, $5.1D^3\gamma'$ and $5.0D^3\gamma'$. Method proposed by *Senders (2008)* has a better slope, since the response is lower at the beginning and more steep at the end of the installation, therefore is following the experimental trend.

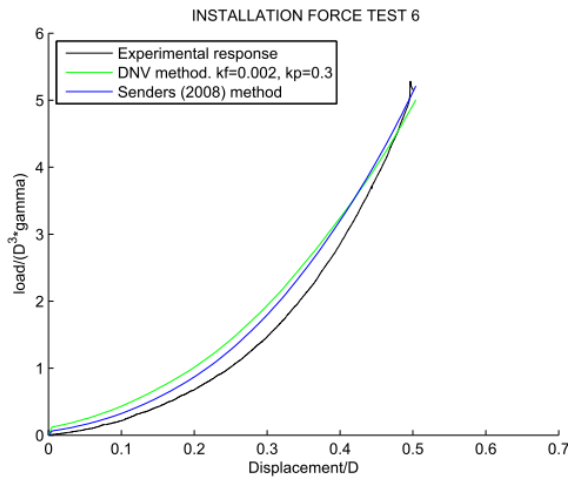


Figure 26. Comparison of DNV and *Senders (2008)* CPT-based methods.

Validation of pull-out CPT-based methods.

CPT-based method proposed in *CUR* is using a $k_f = 0.004$ (*Senders 2008*) that is heavily overestimating the

experimental response, as shown in Figure 27. This is an expected results, inasmuch in *CUR* is presented also an installation method where is used a k_f greater than the one fitted in the previous section. Therefore methods presented in *CUR* are overestimating both installation and pull-out responses.

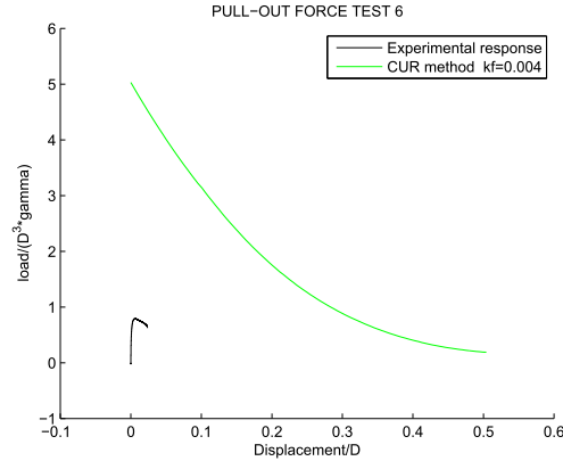


Figure 27 pull-out method presented in *CUR*, heavily overestimate the pull-out resistance.

It is chosen to find another value of k_f , based on the ratio between tensile and compressive friction. $k_f=0.003$, (Table 3), is multiplied for tensile/compressive friction and it is obtained a $k_f = 0.00049$, that is giving a good approximation of the pull-out load for tests without overburden pressure. As can be seen in Figure 28, modified *CUR* method has a peak value of $0.785D^3\gamma'$ where the experimental result is $0.795D^3\gamma'$.

In test with 0kPa overburden pressure, CPT-based method proposed by *Senders (2008)* gives a slight overestimation of the pull-out resistance, due to the greater value of $k_f=0.00053$. As shown in Figure 28, *Senders (2008)* method reaches a peak value of $0.832D^3\gamma'$. This result is slightly unconservative but, since the method does not need any fitting of parameters, method presented in *Senders (2008)* is considered the most reliable CPT-based method to evaluate pull-out resistance.

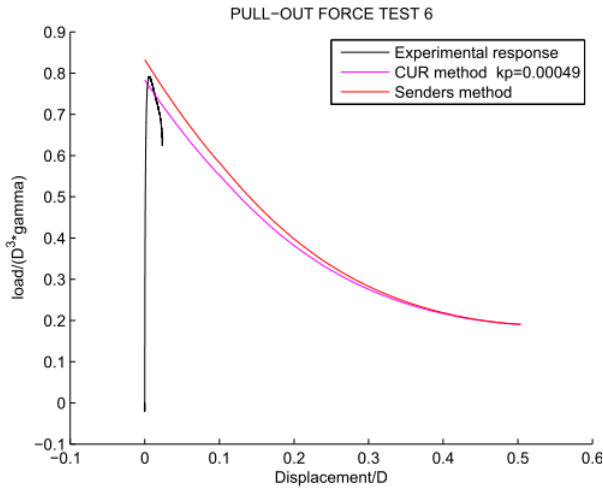


Figure 28 CPT-based method for test without overburden pressure.

In test where overburden pressure is applied, values of cone resistance are evaluated only before of the installation phase. After the application of overburden pressure, q_c is varying and, at this stage, is not possible to carry out the CPT test. Therefore k_f values for test where overburden pressure is applied are fitted in formulae where q_c is measured without overburden pressure. In test where 20kPa and 40kPa of overburden pressure are applied, k_f are evaluated as, respectively, 4.5 and 5.7 times the k_f with zero overburden pressure. Function is fitted in order to evaluate k_f with different overburden pressures (Figure 29). As can be noticed from Figure 29, k_f has a steep increase from 0kPa to 10kPa, therefore where low stress level and high friction angle are present. The slope progressively decreases with the increase of overburden pressure, showing that k_f is not constant but dependent on the applied overburden pressure. As overburden pressure is applied, it is expected a decrease of the friction angle, therefore it is suggested that k_f could be dependent on this latter parameter, but no data are available to confirm this theory.

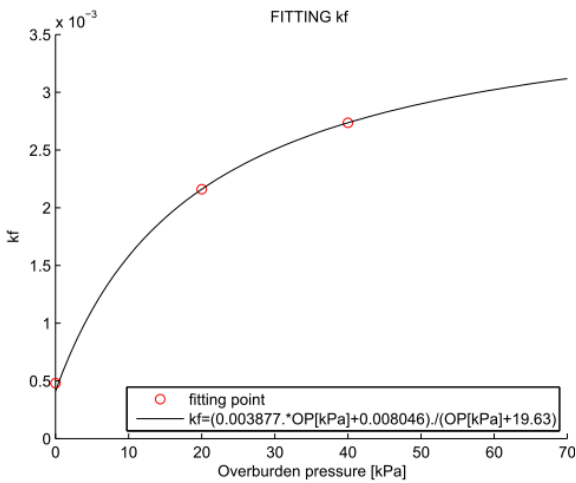


Figure 29 Function relating k_f and overburden pressure.

In Figure 30 and Figure 31 experimental responses are compared with methods results where k_f is evaluated following the curve in Figure 29. Methods are not applied properly, since as previously mentioned, q_c response is not measured after the application of overburden pressure. Therefore k_f approximation in Figure 29 has to be intended as an adaptation of CPT-based methods to the experimental apparatus of Aalborg University, not suitable for a more general application. Results in Figure 30 and Figure 31 are showing that CUR and Senders (2008) methods are respectively underestimating and overestimating the response. Therefore the same trend of zero overburden pressure response is maintained.

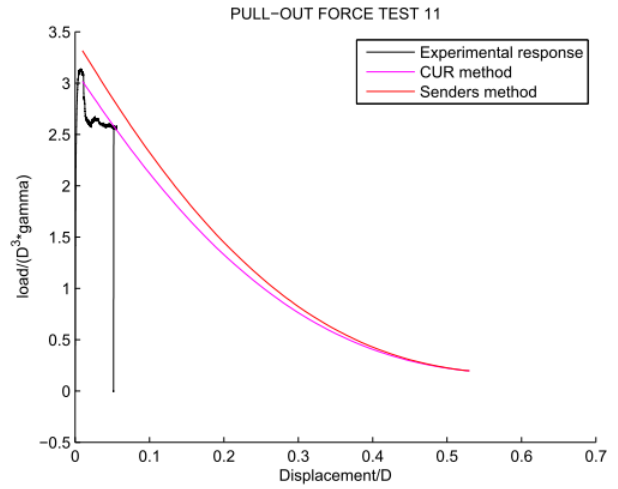


Figure 30 CPT-based methods for 20kPa overburden pressure.

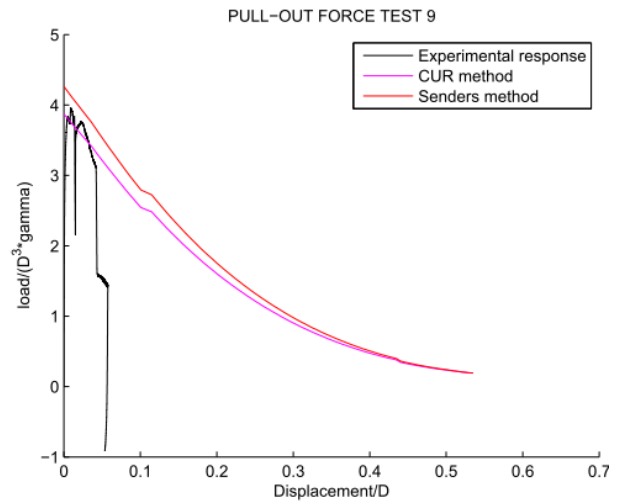


Figure 31 CPT-based methods for 40kPa overburden pressure.

5.4 Validation of beta methods.

Beta methods cannot be used for tests where overburden pressure is applied, since parameters of the soil are unknown. Therefore beta methods are validated only for test where overburden pressure is not applied.

Validation of pull-out beta methods.

To verify beta methods proposed by *Houlsby et al. (2005b)*, first the coefficient of lateral earth pressure K is fitted in the linear method. K is the only unknown, and the linear method is expected to overestimate the pull-out resistance, since is ignoring the reduction of the stress given by skin friction.

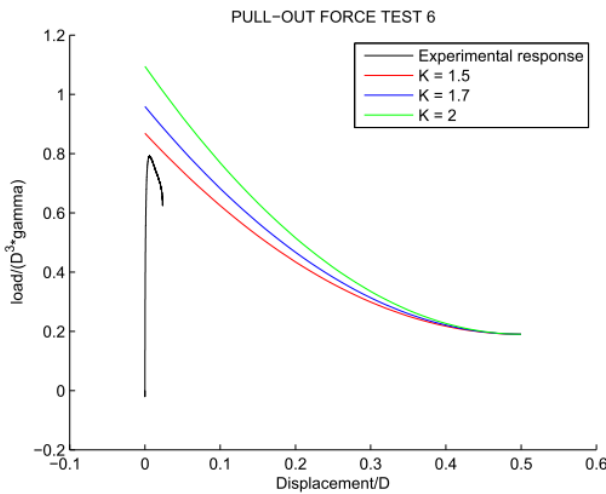


Figure 32 linear method response varying K .

All three responses plotted in *Figure 32* are overestimating the experimental response. Given that is not known how much the linear method should overestimate the experimental response, in order to estimate K it is analyzed the sensitivity of the method proposed by *Houlsby et al. (2005b)* with respect to the variation of parameter m .

In *Figure 33* are shown responses obtained maintaining constant $K=1.5$ and varying the parameter m . Analyzing *Figure 33* it can be seen that increasing m , the reduction in vertical stresses decreases. This means that increasing the volume where upward skin friction is interacting with vertical stress, brings to a smaller total decrease of vertical stress. As can be seen the improvement of the response is higher from $m=1.5$ to $m=2$ with respect to the improvement obtained from $m=2$ to $m=3$, despite Δm is higher in the latter case. This trend is maintained also for higher values of m , and increasing the parameter m convergence with $K=1.5$ is not possible.

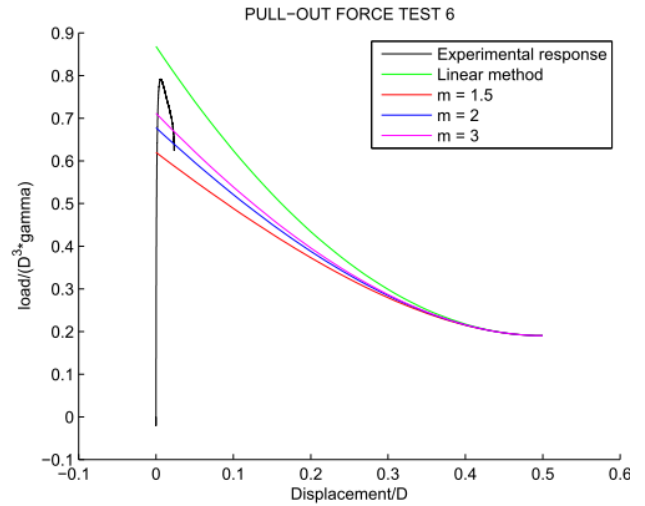


Figure 33 *Houlsby et al. (2005b)* method response, varying m maintaining constant $K=1.5$.

Same considerations made for *Figure 33* can be made for *Figure 34*, where method suggested by *Houlsby et al. (2005b)* is implemented maintaining constant $K=1.7$ and varying m .

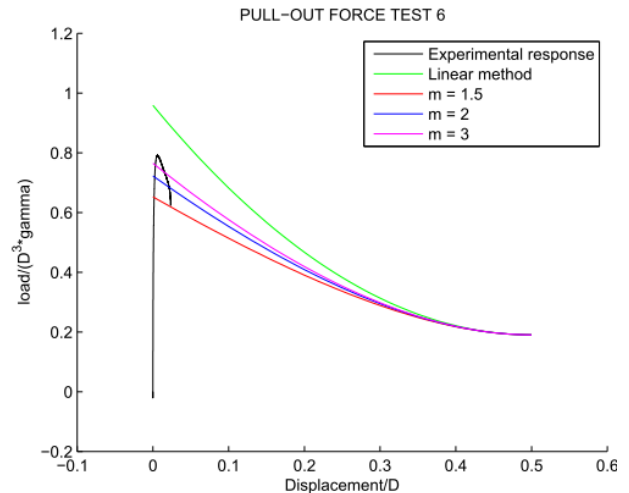


Figure 34 *Houlsby et al. (2005b)* method response, varying m maintaining constant $K=1.7$.

It is chosen to implement the second method maintaining a constant value of $K=2$, and varying the coefficient m in order to find the best fit, as shown in *Figure 35*.

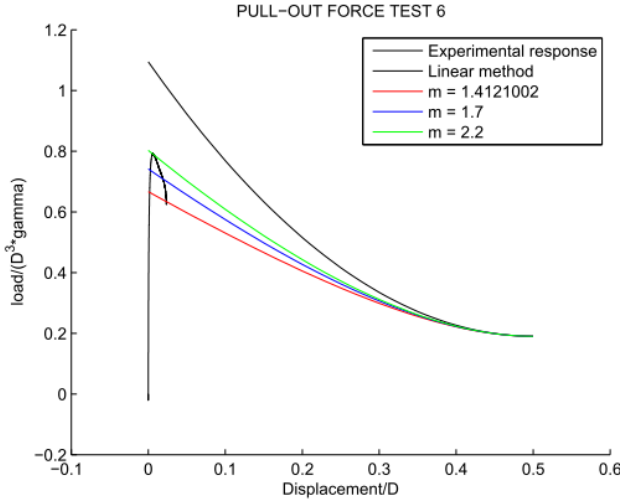


Figure 35 Housby et al. (2005b) method response, varying m maintaining constant $K=2$.

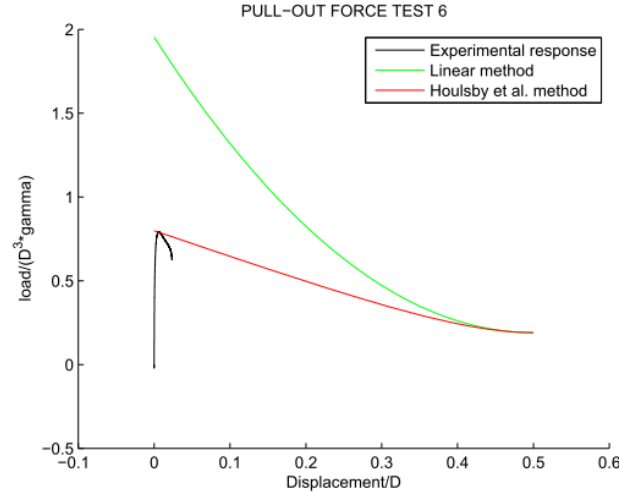


Figure 37 beta method responses, constant used are $m=1.4121002$ and $K=3.9$, reproducing a symmetrical distribution of vertical stress.

Referring to Figure 35, it is assumed that $m=2.2$ is a suitable value to implement this beta method.

In Figure 36 beta methods are plotted with constant $K=2$ and $m=2.2$, giving the best fit. Housby et al. (2005b) method gives a good approximation with a peak value of $0.8D^3\gamma'$, where the experimental response is $0.79D^3\gamma'$. Linear method reaches a value of $1.1D^3\gamma'$ overestimating the experimental response of $0.3D^3\gamma'$.

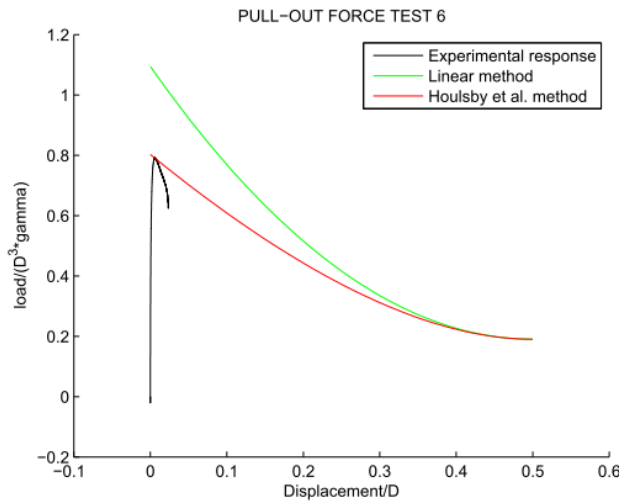


Figure 36 Comparison between the two beta-methods considered, constant used are $m=2.2$ and $K=2$.

It is considered of interest fitting K value when external and internal reduction of vertical stress is symmetrical, therefore with $m=1.4121002$. The response is shown in Figure 37.

Fitted value of $K=3.9$ is considered too high for the examined case. Therefore it can be argued that, following the presented method, a symmetrical distribution of forces is not plausible, and frictional forces are affecting vertical stress in a heavily way on the inside of the skirt.

It has been chose to implement a third pull-out method, following the same idea of the third installation method presented in Housby et al (2005a), where enhancement in vertical stresses is increasing linearly with the depth. To implement the third pull-out beta method, decrease in vertical stresses due to skin friction is increasing inversely proportional with the depth. Z_i and Z_o are calculated with Formulae 12 and 13, then vertical stresses are calculated by means of Formulae 27 and 28. To solve these latter formulae there is not an analytical solution, therefore a fourth order Runge-Kutta method is employed.

$$\frac{d\sigma'_{vi}}{dz} = \gamma' - \frac{\sigma'_{vi}}{Z_i} \quad (27)$$

$$\frac{d\sigma'_{vo}}{dz} = \gamma' - \frac{\sigma'_{vo}}{Z_o} \quad (28)$$

Skin friction is decreasing vertical stress, when this decrease become equal to the vertical stress the soil fails, and vertical stresses become negative, pushing out the caisson from the soil. This behaviour is not realistic, therefore a limitation is introduced, not allowing negative vertical stresses. Therefore decrease in vertical stresses due to skin friction has the geometry shown in Figure 38, where is shown a suction caisson during the pull-out phase and soil affected by skin friction is highlighted.



Figure 38. Geometry of decrease in vertical stresses due to skin friction during pull-out, following the third pull-out beta method.

Response of the third pull-out beta method is shown in Figure 39. Fitting is reached with $f_o=0.8$, $f_i=0.7$, and $K=1.38$.

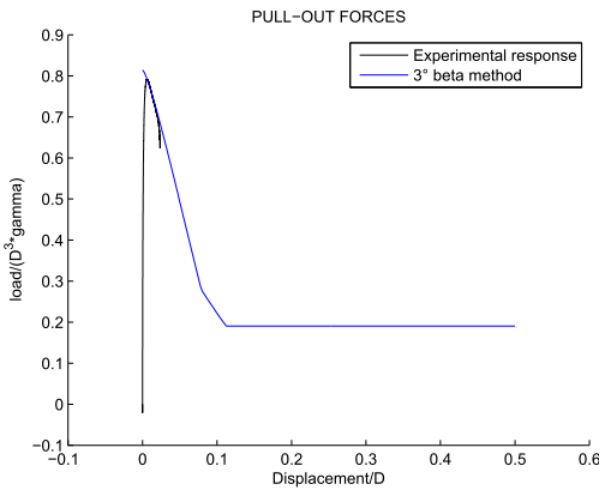


Figure 39. response of third pull-out beta method.

This method is giving a good approximation of the peak resistance, that is $0.8D^3\gamma'$, where the experimental response is $0.79D^3\gamma'$. As can be seen from Figure 39, at a displacement of $0.11D$ the response become horizontal because of the limitation on the negative vertical stress. Therefore for displacements greater than $0.11D$ pull-out resistance is reduced to the weight of the caisson. Since the pull-out experimental data are available only for $45mm$, it is not possible to state that $0.11D$ is the real displacement at which the soil fails. Despite that, the response is showing a good approximation of the available data after the peak.

Validation of installation beta methods.

Installation beta methods are heavily affected on how end bearing factors N_q and N_γ are evaluated.

Larsen (2008) presented formulae to evaluate N_q and N_γ parameters for circular rough foundation. Convergence with these parameters is not possible, as can be seen from Figure 40, where is shown the response obtained with $K=0.8$ and $m=2$.

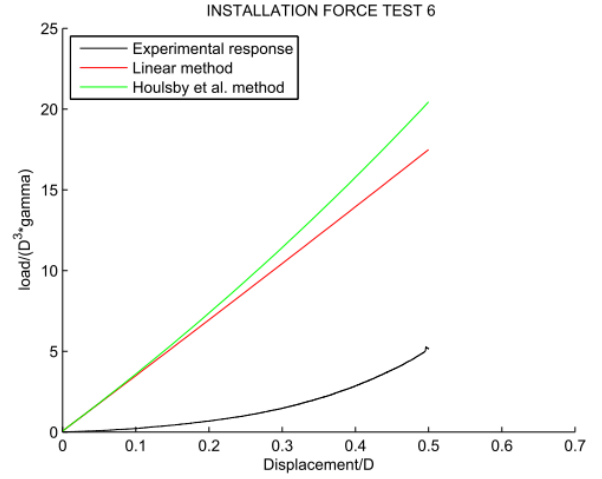


Figure 40. Beta methods implemented with N_q and N_γ from Larsen (2008). $K=0.8$ and $m=2$.

As can be seen in Figure 40, the linear method is heavily overestimating the experimental response, and, consequently, also Houlsby et al. (2005a) method.

It has been chosen to use $N_q = e^{\pi \tan \phi} \tan^2(45 + \phi/2)$ evaluated from Prandtl (1920), and $N_\gamma = 1/4((N_q - 1) \cos \phi)^{1/2}$ according to DS 415 (1998). Response evaluated with these factors is more realistic as can be seen in Figure 41, since is giving a lower end bearing resistance.

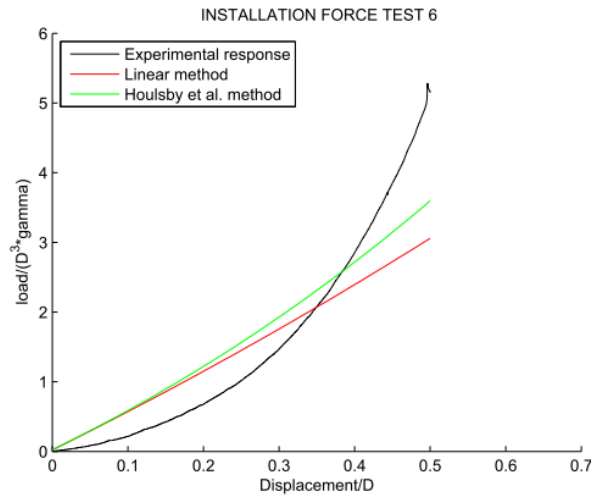


Figure 41. Beta methods implemented with N_q and N_γ according to Prandtl (1920) and DS 415 (1998). $K=0.8$ and $m=2$.

Method proposed by Houlsby et al. (2005a) is dependent on parameters m and K . The parameter m is defining the area affected by friction on the outside of the caisson. This area is an annulus, with internal diameter equal to D_o and external diameter equal to $D_m = D_o * m$, as shown in Figure 42. Inside the skirt, the whole area is considered affected by stress enhancement, and is identified as “internal area” in Figure 42.

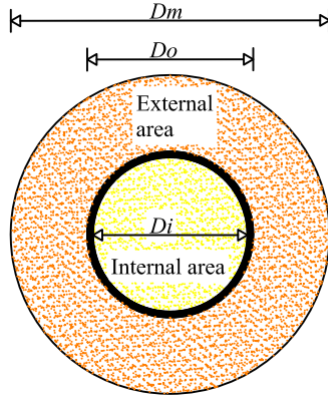


Figure 42. Horizontal section of a suction caisson installed in sand. Internal and external constant areas where stress are affected by friction enhancement are highlighted.

In *Houlsby (2005a)* it is mentioned that for all likely combination of parameters $\sigma'_{vi} \geq \sigma'_{vo}$. It has been noticed that if this condition is satisfied, method proposed by *Houlsby et al. (2005a)* can always been applied.

Considering that the friction force is equal on both sides of the skirt, the enhancement of stress induced by this friction load is larger if the corresponding area is smaller. Therefore the external area has to be greater than the internal area in order to satisfy the condition $\sigma'_{vi} \geq \sigma'_{vo}$. This consideration brings to a limitation of the parameter m , given by *Formula 29*.

$$m \geq \sqrt{\frac{D_o^2 + D_i^2}{D_o^2}} \quad (29)$$

Since vertical stress inside and outside the caisson can differ in magnitude, distribution of stresses at the tip of the skirt can be not symmetrical, and depends on parameter x , (*Formula 8*), as shown in *Figure 43*.

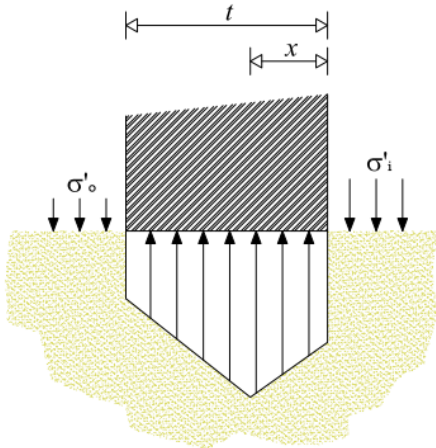


Figure 43. Definition of stress distribution on caisson tip on the basis of method proposed by *Houlsby (2005a)*.

Parameter x defines a length that cannot be neither greater than t nor smaller than zero, as can be deduced from *Figure 43*.

Condition $x \geq 0$ is taken into account in the method proposed in *Houlsby et al (2005a)* by means of *Formula 6* and *Formula 9*. These conditions are considered too strict, since from *Formula 8* it is obtained that $x \geq 0$ is verified also by condition in *Formula 30*.

$$\sigma'_{vi} - \sigma'_{vo} \leq \frac{2\gamma' N_\gamma t}{N_q} \quad x \geq 0 \quad (30)$$

Term on the right side of *Formula 30* is greater with respect to term on the right side of *Formula 6*, therefore *Formula 30* gives a less strict condition.

Beta method presented in *Houlsby et al (2005a)* does not give any specific restriction for $x \leq t$, this condition is satisfied with good approximation if $\sigma'_{vi} \geq \sigma'_{vo}$. Therefore condition of parameter m given by *Formula 29* is used in this work. A less strict and more precise condition is given by *Formula 31*

$$\sigma'_{vi} - \sigma'_{vo} \geq -\frac{2\gamma' N_\gamma t}{N_q} \quad x \leq t \quad (31)$$

As can be noticed from the discussion above, end bearing resistance calculated by means of *Formula 7* is restricted for a relatively small magnitudes of $\Delta\sigma'_v$, with values in a range of $\pm \frac{2\gamma' N_\gamma t}{N_q}$.

In the present work, condition given in *Formula 6* is substituted by less strict condition given in *Formula 30*.

From *Formula 29* it is evaluated the limit value of parameter $m=1.4121002$. Response evaluated with a value of $K=0.8$ suggested by *Senders (2008)*, is shown in *Figure 44*.

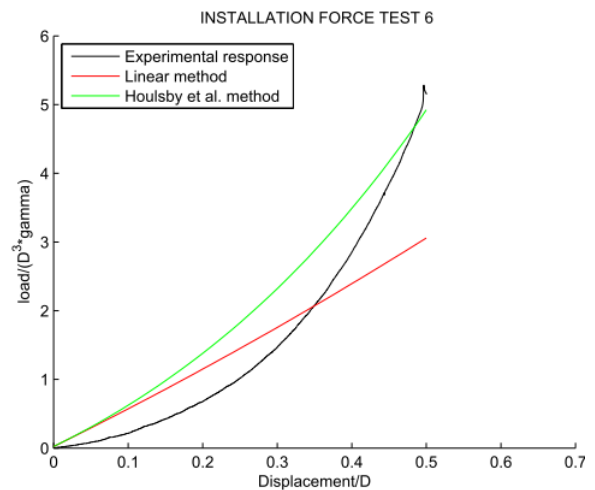


Figure 44. Beta methods, $K=0.8$ $m=1.4121002$.

Response of *Houlsby et al (2005a)* method shown in *Figure 42* gives a peak value of $4.91D^3\gamma'$, where the experimental response is $4.92D^3\gamma'$ therefore the estimated response can be

considered precise. Linear method has a peak value of $3.1D^3\gamma'$ underestimating the experimental response as expected.

When the end bearing resistance is evaluated using the limit value of m , force distribution at the tip of the caisson (*Figure 41*) is symmetrical, since $x=t/2$. Seeing considerations made in the previous section for *Figure 37*, symmetrical distribution of vertical stress is not considered suitable for this method, therefore fitting showed in *Figure 42* is not considered satisfying.

It is chosen to adopt $K=2$, evaluated from pull-out beta methods. Responses where $K=2$ is maintained constant and parameter m is varying are plotted in *Figure 45*.

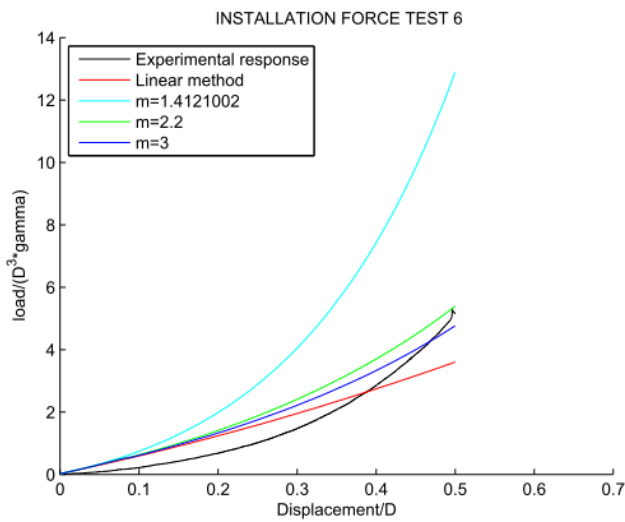


Figure 45. Beta methods responses maintaining constant $K=2$ and varying parameter m .

As can be seen in *Figure 45*, limit value of $m=1.4121002$, representing a symmetrical distribution of enhanced stress, is heavily overestimating the experimental response with a peak value of $12.89D^3\gamma'$. Responses obtained using $m=2.2$ and $m=3$ are giving respectively peak values of $5.4D^3\gamma'$ and $4.71D^3\gamma'$, where the experimental response is $4.92D^3\gamma'$. Result obtained with $m=2.2$ is considered acceptable, since is overestimating the experimental response, therefore is giving a safe approximation of the installation force.

A more precise fitting, shows that response evaluated with $K=2$ and $m=2.46$ gives a better approximation of the experimental result, since reaches a peak value of $5.0D^3\gamma'$, as can be seen in *Figure 46*.

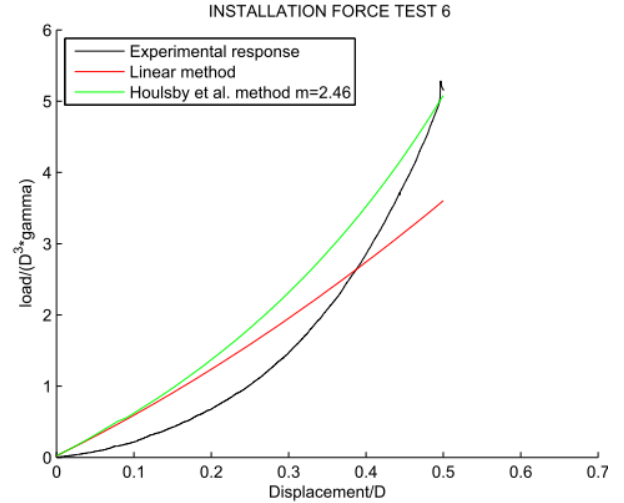


Figure 46. Beta methods, $K=2$, $m=2.46$.

Despite the good fitting shown in *Figure 46*, combination of parameters $m=2.2$ and $K=2$ is considered the most suitable, since is giving good approximation also in the second pull-out beta method proposed by *Houlsby et al.(2005b)*.

Third installation beta method described in *Houlsby et al.(2005b)* is implemented maintaining $K=1.38$ found with the pull-out method. Fitted parameters are $f_o=1.49$ and $f_i=0.7$.

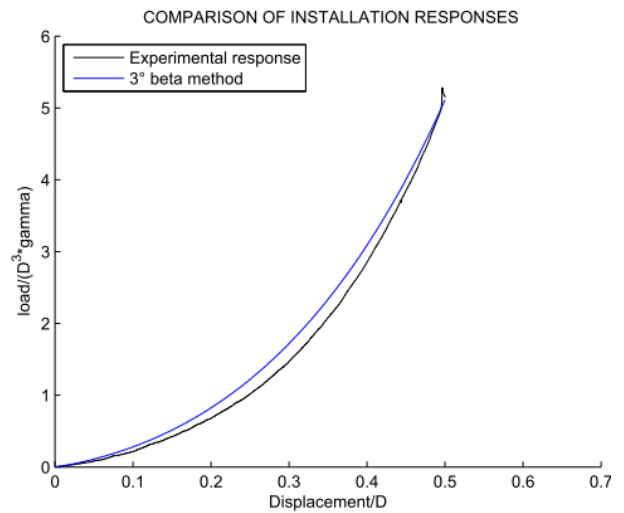


Figure 47. Third beta methods response, $K=1.38$, $f_o=1.49$ and $f_i=0.7$.

As shown in *Figure 47*, this latter beta method is giving a good approximation of the peak installation resistance, giving a value of $5.06D^3\gamma'$ where the experimental response is $4.92D^3\gamma'$. The approximation of the slope is considerably improved with respect others beta methods.

6. CONCLUSIONS.

This article presents a testing rig of Aalborg University, and the procedure followed to carry out tests. Responses obtained are considered of high reliability, given the low scaling factor adopted ($1:10$) and the standardized procedure followed in each test.

The possibility to apply overburden pressure allows examining a wide range of skirt length. This allows extending the possibility of study to configurations otherwise not reachable.

Methods to evaluate pull-out and installation forces are validated, relying on responses obtained from tests described. More tests are needed in order to reach a better definition of parameters on which methods are based.

Since in installation measurements is not well defined where the lid makes contact with soil, an approximation on this value has been done. It is believed that more precise data can be obtained installing for a depth of 50cm the bucket model $M2$ ($L/D=1$). Following this expedient ensures that only frictional forces and end-bearing resistance at the tip of the caisson are present, therefore better parameters can be obtained.

Given that beta methods based on parameter " m " used to evaluate pull-out and installation resistance have been elaborated making approximations, also the parameter $K=2$ found with the second pull-out beta method is affected by these approximations. On the inside of the caisson it is assumed that all the soil is affected by skin friction in the same manner, overestimating the enhancement/reduction of vertical stress. Therefore have a symmetrical distribution of the stress as shown in *Figure 37*, means to overestimate/underestimate vertical stress also outside the caisson. Parameter $m=2.2$ has the physical meaning of a diameter $D_m=2.2\text{m}$ that is affected by skin friction on the outside of the caisson. $D_m=2.2\text{m}$ is clearly an unlikely value, obtained because the effect of the friction on the outside of the caisson has to be underestimated in order to compensate the overestimation of the same effect on the inside of the skirt.

A more precise approximation of installation and pull-out experimental responses are given by the third installation beta method presented in *Houlsby et al (2005b)* and by the solution of the third pull-out beta method presented in this work. Despite a better approximation can be obtained, the latter methods have some restrictions, and cannot be applied to a bucket with $L/D=1$.

CPT based methods are easier to apply and are showing a better approximation of the experimental response with respect to beta methods. Dependence of k_f to overburden pressure has been demonstrated, however a better definition of parameters used in CPT based method is needed.

REFERENCES.

- Byrne, L.B. and Houlsby, G.T. (2003). "Foundation for offshore wind turbines", Phil. Trans. of the Royal Society of London, Series A 361, 2909-2300.
- CUR (2001) 2001-8; Bearing capacity of steel pipe piles, Centre for Civil Engineering Research and Codes.
- DNV (1992) Classification notes No 30.4, Hovik, Det Norske Veritas.
- DS 415 (1998) Norm for fundering (Code of Practice for foundation engineering), 4th. edition, Danish standard Copenhagen, In Danish.
- Fisker, L.B., and Kromann, K. (2004). "Cyklisk Belastning af Bøttefundament i Tryktank", Speciale ved Aalborg University.
- Houlsby, G.T. and Byrne, B.W. (2005a). Design procedures for installation of suction caissons in sand. Proceedings of the ICE, Geotechnical Engineering 158, No. 3, 135-144.
- Houlsby, G. T., Kelly, R. B. & Byrne, B. W. (2005b) The tensile capacity of suction caissons in sand under rapid loading. Proc. International Symposium on Frontiers in Offshore Geotechnics (ISFOG). Perth, Australia, Tayler & Francis Group.
- Houlsby, G.T., Ibsen, L.B., and Byrne, B.W.(2005c) "Suction caisson for wind turbines" Department of Civil Engineering, Aalborg University Denmark, Department of Engineering Science Oxford University UK.
- Hedegaard, J. and Borup, M. (1993). "Data Report Baskarp Sand No 15", Division of Geotechnical and Foundation Engineering, Aalborg University.
- Ibsen L.B., Hanson, M Hjort, T. and Taarup, M. (2009) "MC-Parameter Calibration for Baskarp Sand No. 15" DCE Technical Report No.62. (ISSN 1901-726X), Aalborg University, Department of Civil Engineering, Aalborg, Denmark.
- Larsen K.A. (2008), Static Behaviour of Bucket Foundations, Ph.D. Thesis, Aalborg University, Department of Civil Engineering Division of Water & Soil. Aalborg, Denmark.
- Lehane, B. A., Schneider, J. A. & Xu, X. (2005) The UWA-05 method for prediction of axial capacity of driven piles in sand. Proc. International Symposium 'Frontiers in Offshore Geotechnics'. Perth, Australia, Taylor & Francis Group.
- Kelly, R. B., Houlsby, G. T. & Byrne, B. W. (2006). A comparison of field and laboratory tests of caisson

foundations in sand and clay. *Getotechnique*, 56, No. 9, 617–626.

Prandtl L. (1920) Über die Härte plastischer Körper, *Nachr. D. Ges.D.Wiss*, Göttingen 1920.

Randolph, M.F., Jamiolkowski, M. B. & Zdravkovic, L. (2004) Load carrying capacity of foundations. *Proc. Skempton Memorial Conf.* London.

Senders, M., (2008) Suction Caissons in Sand As Tripod Foundations for Offshore Wind Turbines, Ph.D. Thesis, University of Western Australia.

Sjelmo, Å. (2012) “Soil-Structure Interaction in Cohesionless Soils due to Monotonic Loading”, MSc. Student Report, Department of Civil Engineering, Aalborg University.

Sørensen, S. P. H., M. Møller, K. T., Augustsen A. H. Brødbæk, and L.B. Ibsen, (2009). Evaluation of Load-Displacement Relationships for Non-Slender Monopiles in Sand. DCE Technical Report No. 79. (ISSN 1901-726X), Aalborg: Aalborg University, Civil Engineering Department.

Recent publications in the DCE Technical Memorandum Series

